
VITA: VISION-TO-ACTION FLOW MATCHING POLICY

Dechen Gao¹, Boqi Zhao¹, Andrew Lee¹, Ian Chuang², Hanchu Zhou³, Hang Wang³,

Zhe Zhao¹, Junshan Zhang³, Iman Soltani⁴

¹Department of Computer Science, University of California, Davis

²Department of Electrical Engineering and Computer Sciences, University of California, Berkeley

³Department of Electrical and Computer Engineering, University of California, Davis

⁴Department of Mechanical and Aerospace Engineering, University of California, Davis
dchgao@ucdavis.edu, boqzhao@ucdavis.edu, awclee@ucdavis.edu, ianc@berkeley.edu
hczhou@ucdavis.edu, whang@ucdavis.edu, zao@ucdavis.edu, jzh@ucdavis.edu,
isoltani@ucdavis.edu

July 18, 2025

ABSTRACT

We present VITA, a **V**ision-**T**o-**A**ction flow matching policy that evolves latent visual representations into latent actions via flow matching for visuomotor control. Traditional flow matching and diffusion policies face a fundamental inefficiency: they sample from standard source distributions (e.g., Gaussian noise) and then require additional conditioning mechanisms, such as cross-attention, to condition action generation on visual information, incurring time and space overheads. We propose VITA, a novel paradigm that treats latent images as the source of the flow, and learns an inherent mapping from vision to action. VITA eliminates the need for separate conditioning modules, while preserving the generative modeling capabilities. However, learning the flow between fundamentally different modalities, such as vision and action, can be intrinsically challenging. Action data is sparser and lacks semantic structures. Additionally, visual representations are typically much higher-dimensional than raw actions, while flow matching requires the source and target to have identical shapes. To resolve this, we propose to create a structured action latent space via an autoencoder as the target for flow matching, and up-sample raw actions to latent actions to match visual representation shapes. We also show it is crucial to supervise flow matching not only with encoder targets, but also with the final action outputs. We propose flow latent decoding, to backpropagate action reconstruction loss through sequential flow matching ODE (ordinary differential equations) solving steps, enabling effective end-to-end learning. We implement VITA as simple MLP layers, and evaluate VITA on challenging bi-manual manipulation tasks on the ALOHA platform, including 5 simulation and 2 real-world tasks. Despite its simplicity, MLP-only VITA outperforms or matches state-of-the-art generative policies, while reducing inference latency by 50% to 130% compared to conventional flow matching policies requiring different conditioning mechanisms or complex architectures. To our knowledge, VITA is the first MLP-only flow matching policy capable of solving complex bi-manual manipulation tasks like those in ALOHA benchmarks. Project page: [VITA](#).

Keywords Imitation Learning · Flow Matching · Robotics Manipulation · Policy Learning

1 Introduction

Flow matching, a generalization of diffusion, has demonstrated remarkable success across a wide range of cross-modal generation tasks, from text-to-image generation [1, 2, 3, 4, 5, 6], text-to-video generation [7, 8, 9], to visuomotor (vision-to-action) policy [10, 11, 12, 13, 14, 15, 16, 17]. Conventional flow matching and diffusion methods generate

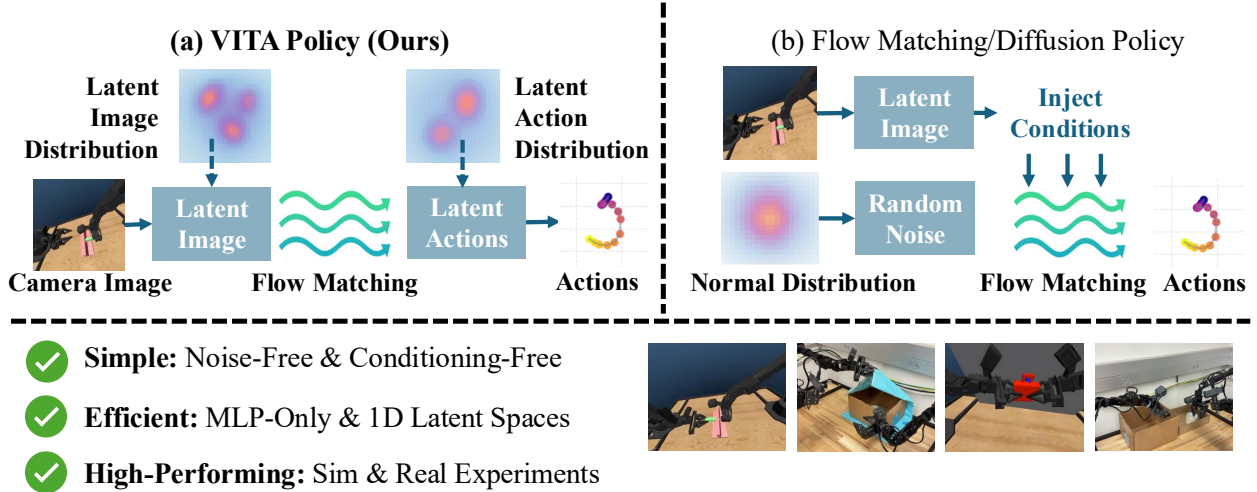


Figure 1: An overview of VITA—a noise-free, conditioning-free policy learning framework. Unlike conventional flow matching and diffusion policies that rely on sampling from standard distributions and require extra conditioning modules (e.g., cross-attention), VITA learns a continuous flow from latent visual representations to latent actions. By leveraging compact 1D visual and action latent spaces, and eliminating additional conditioning modules, VITA enables a highly efficient MLP-only architecture, achieving strong performance and inference efficiency across both simulation and real-world visuomotor tasks.

samples in the target modality by starting from a simple source distribution (often Gaussian) and progressively “denoising” them into the target modality distribution [18, 19]. To condition generation processes based on source modality inputs, conventional flow matching or diffusion necessitate additional conditioning mechanisms, e.g., cross-attention [1, 6, 10, 20], to inject source modality inputs at each denoising step, adding further complexity to both implementation and runtime overheads [4, 5].

In robot learning contexts specifically, minimizing policy inference latency and memory footprint is critical for effective real-time control. To overcome the computational inefficiencies inherent to conventional flow matching and diffusion policies, we introduce VITA (VIision-To-Action flow matching), a noise-free policy learning framework that directly connects the visual and action latent distributions. Unlike conventional approaches that rely on Gaussian noise priors and additional conditioning mechanisms, VITA leverages the flexibility of flow matching—which places no constraints on the source distribution—to treat latent image representations as the source distribution for the flow. These latent images inherently encode the visual context required for visuomotor tasks, thus eliminating the need for additional conditioning modules. VITA significantly reduces inference latency and memory overhead, simplifying the overall network architecture.

Learning vision-to-action flow matching presents several unique challenges. Bridging two distinct modalities is inherently difficult [4, 5], particularly in robot learning contexts where action data is often limited, unstructured, and sparse, whereas the visual representations feature rich structures and semantics, and have far more dimensions. Additionally, flow matching demands the source and target distributions to have identical shapes. To address these issues, we propose two crucial designs in VITA. First, we introduce a structured latent action space, learned via an action autoencoder, that allows action representations to match the dimensionality of visual representations and serves as a structured and tractable target distribution for flow matching. Specifically, the action encoder transforms raw actions into latent action targets for flow matching, while the decoder translates these latent actions back into raw actions. However, unlike latent diffusion models for image generation [1]—which leverage abundant image data to pre-train latent image spaces and subsequently freeze them as fixed flow matching targets—a fixed, pre-trained latent action space yields poor performance for vision-to-action flow, due to the inherent sparsity and limited amount of action data available to train a reliable latent action representation. To overcome this limitation, our second key design enables end-to-end joint learning of both the flow matching and latent action space by backpropagating gradients through the ordinary differential equations (ODE) solving steps. This differentiates VITA fundamentally from existing cross-modal generation approaches, e.g., latent diffusion or flow matching models for image generation [1, 5, 4, 21], which fix the target distribution when training flow matching or diffusion models. We found that for vision-to-action flow matching learning, fixed targets yield poor performance, and enabling gradient updates through ODE solving for fully end-to-end training is crucial for achieving superior performance with VITA.

We evaluate VITA on both real-world and simulated tasks using the ALOHA [22, 23, 24] platform. Our experiments demonstrate that VITA consistently outperforms or matches state-of-the-art generative policies. We instantiate VITA with only MLP layers for the flow matching network and action decoder, complemented by 1D latent representations. Compared to state-of-the-art flow matching and diffusion policies that predominantly leverage complex architecture such as transformers [2, 3] or U-Net [25, 10], and introduce conditioning modules [20, 10, 26, 14], the MLP-only and noise-free VITA policy achieves, e.g., 50% to 130% reduction in inference latency compared to conventional flow matching. To our knowledge, **VITA is the first MLP-only flow matching policy to succeed on tasks as challenging as ALOHA bi-manual manipulation.** By harnessing the unique strengths of flow matching, VITA paves the way for a new paradigm in visuomotor learning that is both conceptually elegant and practically efficient, unifying perception and control in a noise-free, conditioning-free generative manner.

Our main contributions are summarized as follows:

- **A Noise-Free Visuomotor Learning Paradigm.** We propose VITA, which evolves latent visual representations into latent actions via flow matching without sampling from simple noise distributions. By treating vision as the source distribution, our method obviates costly conditioning mechanisms, like cross-attention, which are adopted by conventional diffusion and flow matching policies.
- **A Simple and Efficient Policy Architecture.** We demonstrate the effectiveness of an MLP-only architecture for flow matching parameterization in complex, high-dimensional control. VITA uses 1D visual representations and generates 21-DoF continuous actions with simple MLP, proving that complex or resource-intensive networks such as transformers are not a prerequisite for high-performance generative policies. To our knowledge, VITA is the first MLP-only flow matching parameterization to master tasks challenging as ALOHA bi-manual manipulation.
- **State-of-the-Art Performance in Real and Simulated Environments.** VITA surpasses state-of-the-art generative policies in success rates while being significantly more efficient. Specifically, our design reduces inference latency by 50% to 130% compared to conventional flow matching. We also verify the effectiveness of VITA in real-world experiments on ALOHA.

2 Related Work

2.1 Imitation Learning for Visuomotor Policy.

Imitation learning enables robots to learn complex behaviors by mimicking expert demonstrations. Behavioral cloning, a prominent imitation learning paradigm, frames this as a supervised learning problem, learning a policy that maps observations to actions [26, 27]. Recent advancements in behavioral cloning have been heavily influenced by two modeling approaches: generative modeling and autoregressive modeling. Generative methods learn a conditional distribution of actions given an observation. This category includes policies based on conditional variational autoencoders (CVAEs) [26, 27], as well as diffusion [20, 10] and flow matching [28, 14]. On the other hand, autoregressive approaches tokenize actions and frame policy learning as a sequence modeling task. These methods predict action tokens sequentially, using next-token prediction [29], next-scale prediction [30], or bi-directional prediction [13]. Generative models ubiquitously require extra conditioning modules (e.g., cross-attention [20], AdaLN [20], FiLM [31, 10]) to inject observations at each step of the generation process. Furthermore, top-performing policies in both the generative and autoregressive paradigms commonly employ large, expressive networks such as U-Nets or transformers to succeed on complex, high-dimensional robotics tasks. VITA diverges from these trends by addressing these inefficiencies directly. By formulating the policy as a noise-free vision-to-action flow from a 1D visual latent representation to a 1D action latent representation, VITA entirely removes the need for additional conditioning mechanisms. The 1D latent representations enable the use of a simple and efficient MLP-only network for flow matching parameterization, even for challenging bi-manual manipulation tasks.

2.2 Diffusion and Flow matching for Generative Modeling.

Diffusion [32], grounded in stochastic differential equations (SDEs), generates complex data distributions by sampling from a simple source distribution (typically Gaussian) and iteratively denoising it to the target distribution [19]. Flow matching [18, 33] has been proposed to enable faster training and sampling [33, 34, 35, 18] by modeling the map between source and target distributions with an ordinary differential equation (ODE). Both diffusion and flow matching models have shown strong performance across diverse generative tasks, such as image generation [1, 2, 3, 6, 36, 37], video generation [7, 8], and visuomotor policies [10, 20, 17, 38]. Unlike diffusion, flow matching theoretically places no constraints on the choice of source distribution [34], and a few works have explored leveraging this property to learn the direct transport within the same modality [39, 40], e.g., for image-to-image generation tasks [41, 42], recently,

CrossFlow [4] and FlowTok [5] extended this to more challenging cross-modal generation between text and image. VITA focuses on learning to bridge vision and action for visuomotor control, where the target modality, action, features sparser data, and lacks semantic structures, compared to text or images, presenting unique challenges. Different from flow matching for image generation, which typically pre-trains and freezes the image encoder and decoder when learning flow matching or diffusion models for image generation [1, 5, 4], VITA resorts to a fully end-to-end pipeline training to effectively learn the latent action space from limited and sparse action data. We propose to enable effective end-to-end learning by backpropagating a flow latent decoding loss through ODE solving steps during training.

3 Preliminaries

Flow matching models learn to transport samples from a source probability distribution p_0 to a target distribution p_1 by learning a velocity vector field v_θ [18, 43]. This generative process is defined by an ordinary differential equation (ODE):

$$\frac{dz_t}{dt} = v_\theta(z_t, t)$$

where $t \in [0, 1]$ is a continuous time variable, z_t represents a sample at time t , and the model v_θ is a neural network. The goal of training is for v_θ to generate a path that transforms a sample $z_0 \sim p_0$ into a corresponding sample $z_1 \sim p_1$.

For a simple, straight probability path between two samples, the interpolated state at time t is defined as:

$$z_t = (1 - t)z_0 + tz_1$$

The corresponding ground-truth velocity of this path given by $u_t = \frac{dz_t}{dt} = z_1 - z_0$. The network v_θ is trained by minimizing the Mean Squared Error (MSE) between its predicted velocity and the ground-truth velocity:

$$\mathcal{L}_{\text{FM}} = \mathbb{E}_{t, z_0, z_1} \left[\|v_\theta(z_t, t) - (z_1 - z_0)\|^2 \right] \quad (1)$$

During inference, starting from a source sample z_0 , the model generates a target sample \hat{z}_1 by solving the ODE initial value problem from $t = 0$ to $t = 1$:

$$\hat{z}_1 = z_0 + \int_0^1 v_\theta(z_t, t) dt$$

Notably, conventional flow matching or diffusion policies for visuomotor control generate actions by evolving a sample from a simple prior distribution, such as Gaussian noise ($z_0 \sim \mathcal{N}(0, I)$), and require conditioning on visual inputs to guide the generation process [28, 10, 20]. However, flow matching does not assume the source distribution must be simple noise; it can theoretically connect two arbitrary distributions. We exploit this flexibility to re-formulate generative visuomotor policy learning: we directly use the latent distribution of visual observations as the source distribution p_0 , yielding a noise-free flow matching process that eliminates the need for costly conditioning modules and therefore boosts time and space efficiency.

4 VITA: Vision-to-Action Flow Matching

In this section, we detail the core designs of the VITA flow matching policy. We begin by formulating VITA flow matching (Section 4.1), and providing a high-level overview of VITA architecture (Section 4.2). Next, we explain why the creation of a latent action space is a critical design choice (Section 4.3). Finally, we outline the training objectives that enable fully end-to-end optimization of both flow matching and the action autoencoder from scratch, with a particular focus on the "flow latent decoding" technique that backpropagates through ODE solving steps and facilitates effective learning from limited and sparse expert data (Section 4.4).

4.1 Flowing from Vision to Action

VITA learns a policy $\pi(A|O)$ that maps observations O to a corresponding sequence of future actions A . Observations (O) represent observations from the environment, which include raw images $I \in \mathbb{R}^{H \times W \times C}$ and, optionally, the robot's proprioceptive state vector S . Actions (A) represent a sequence of actions over a future prediction horizon, defined as $A \in \mathbb{R}^{T_{\text{pred}} \times D_{\text{action}}}$, where T_{pred} is the prediction horizon and D_{action} is the dimensionality of the action space. We use action chunking ($T_{\text{pred}} > 1$) for better temporal consistency [26].

Unlike conventional flow matching policies that generate actions from a random noise vector conditioned on visual inputs, VITA formulates the visuomotor policy as learning a vision-to-action flow between the source distribution of

latent visual representations (p_0) and the target distribution of latent actions (p_1) without extra conditioning on visual inputs. The flow matching learns to evolve a visual latent representation z_0 into an action latent representation z_1 by learning a velocity field $v_\theta(z_t, t)$. Notably, z_0 and z_1 are required to have the same shape in flow matching, which necessitates learning a latent action space to match the dimensionality of visual inputs (Section 4.3).

During inference, the current observation O_{curr} is encoded into its visual latent representation $z_0 = \mathcal{E}_v(O_{\text{curr}})$. Next, this latent vector is evolved into a predicted action latent representation, \hat{z}_1 , by numerically solving the ODE from $t = 0$ to $t = 1$ using the learned velocity field v_θ :

$$\hat{z}_1 = z_0 + \int_0^1 v_\theta(z_t, t) dt \quad (2)$$

In other words, \hat{z}_1 is obtained by numerically solving the flow matching ODE, and serves as an approximation to the target latent z_1 . Finally, the resulting latent action vector \hat{z}_1 is passed through the action decoder to produce the final action chunk:

$$\hat{A} = \mathcal{D}_a(\hat{z}_1)$$

4.2 VITA Architecture Design

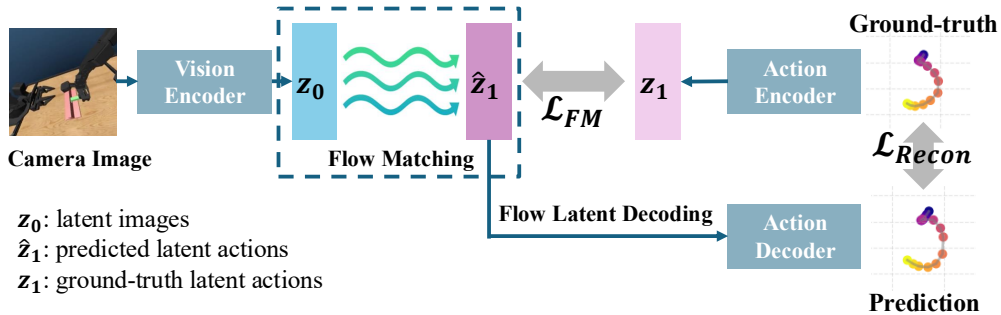


Figure 2: An overview of the VITA architecture. The Vision Encoder processes observations into a source latent representation z_0 for the flow. The Action Encoder provides a target latent representation z_1 for flow matching training. The Action Decoder translates \hat{z}_1 (latent actions generated by solving ODEs) or z_1 (latent actions from action encoder) back to raw action chunks. The MLP-based flow matching network learns the velocity field to evolve z_0 into \hat{z}_1 over a continuous flow matching path.

As depicted in Figure 2, the VITA architecture is composed of the following three primary neural network components: **Vision Encoder** (\mathcal{E}_v), **Action Autoencoder** (Encoder \mathcal{E}_a , and Decoder \mathcal{D}_a), and **Flow Matching Network** (v_θ).

The **Vision Encoder** (\mathcal{E}_v) maps raw camera images into a 1D visual latent representation I . The observation O to the policy consists of both 1D image representations I and, optionally, the robot’s proprioceptive states S . We use a simple MLP to project the O into a flattened latent representation $z_0 = \mathcal{E}_v(O)$, where $z_0 \in \mathbb{R}^{D_{\text{latent}}}$. In our experiments, we set $D_{\text{latent}} = 512$ for all the tasks.

The **Action Autoencoder** learns a compact representation for action sequences. Its **Action Encoder** (\mathcal{E}_a) maps the ground-truth action chunk A to the latent action $z_1 = \mathcal{E}_a(A)$, where $z_1 \in \mathbb{R}^{D_{\text{latent}}}$. The corresponding **Action Decoder** (\mathcal{D}_a) is an MLP that reconstructs an action chunk $\hat{A} = \mathcal{D}_a(\hat{z}_1)$ from a predicted latent action \hat{z}_1 .

Finally, the **Flow Matching Network** (v_θ) parameterizes the velocity field of the flow. By design, our source and target representations (z_0, z_1) are 1D vectors, which allows the velocity field to be modeled effectively with a simple MLP. This approach avoids the computational overhead associated with more complex mechanisms like self-attention or cross-attention, which are common in other generative policies [10, 20, 26, 30].

4.3 Latent Action Spaces as Flow Matching Target Distributions

In typical visuomotor tasks, visual representations are significantly higher-dimensional than raw action chunks. For instance, the actions are 21-dimensional per time step on challenging AV-ALOHA bi-manual manipulation tasks, while vision encoders can produce feature vectors of, e.g., 512 dimensions per image [24, 20, 26, 10], or even higher dimensions when using 2D vision tokenizers [10].

Flow matching requires the inputs and targets to have identical shapes. To satisfy this constraint, one option is to down-sample latent image representations to the action chunk shape, which, however, can cause aggressive compression and

severe information loss. Instead, VITA chooses to up-sample action chunks to higher-dimensional action representations to match the latent image shape. VITA implements an action autoencoder to project action chunks to a latent action space. In Section 5.3, we will show that learning a well-structured latent space as the target distribution via an autoencoder for flow is crucial for the success of VITA, particularly in the context of limited and sparse action data.

4.4 VITA Learning

The VITA policy is trained end-to-end from scratch. The learning process is governed by a composite objective consisting of the following three primary losses.

The first objective is the **Flow Matching Loss** (\mathcal{L}_{FM}), defined in Equation (1), which operates purely in the latent spaces. It supervises the MLP-based flow network v_θ to accurately predict the velocity vectors that gradually transport the visual latent representations z_0 to their corresponding action latent representations z_1 over a continuous time horizon.

The most critical objective in VITA is the **Flow Decoding Loss** (\mathcal{L}_{FD}). Unlike conventional cross-modal generation methods—such as latent diffusion models for image generation [1, 4, 5]—which rely on a fixed target distribution obtained via pre-trained and frozen image encoders and decoders, the sparsity and limited availability of action data can make it difficult to learn a well-structured latent action space suitable as a fixed flow target. To overcome this, VITA introduces flow decoding loss to enable effective end-to-end training of both the flow matching network and the action autoencoder jointly. While \mathcal{L}_{FM} ensures accurate velocity prediction in the latent space, it does not directly guarantee that the final latent action vector \hat{z}_1 , obtained via solving flow matching ODEs, will decode into a high-quality action. To bridge this gap, \mathcal{L}_{FD} decodes the predicted action latent \hat{z}_1 and computes a reconstruction error against the ground-truth action A .

$$\mathcal{L}_{\text{FD}} = \|\mathcal{D}_a(\hat{z}_1) - A\|, \quad \text{where } \hat{z}_1 = z_0 + \int_0^1 v_\theta(z_t, t) dt$$

In practice, this integral is approximated numerically using an efficient, Euler ODE solver. This objective provides a direct, end-to-end supervision signal that propagates gradients from the final action space back through the action decoder, the flow matching network, and the vision encoder, across multiple ODE steps. This ensures the entire model is optimized to produce latent representations that are not only correctly positioned in the flow field but are also decodable into accurate actions.

Finally, the **Action Autoencoder Loss** (\mathcal{L}_{AE}) can help create a well-structured action latent space. This objective primarily consists of a reconstruction loss, $\mathcal{L}_{\text{recon}} = \|\mathcal{D}_a(\mathcal{E}_a(A)) - A\|$, which trains the autoencoder to accurately map action sequences to and from the latent space.

$$\mathcal{L}_{\text{recon}} = \|\mathcal{D}_a(\mathcal{E}_a(A)) - A\|$$

When a variational autoencoder (VAE) is used [44], an optional KL-divergence loss, $\mathcal{L}_{\text{KL}} = D_{\text{KL}}(q(z_1|A) \| p(z_1))$, can be added. This term regularizes the posterior distribution of the action encoder, $q(z_1|A)$, encouraging it to approximate a standard Gaussian prior, $p(z_1) = \mathcal{N}(0, I)$.

$$\mathcal{L}_{\text{KL}} = D_{\text{KL}}(q(z_1|A) \| p(z_1)), \quad p(z_1) = \mathcal{N}(0, I)$$

The final training objective is a weighted sum of these losses:

$$\mathcal{L}_{\text{VITA}} = \lambda_{\text{FM}}\mathcal{L}_{\text{FM}} + \lambda_{\text{FD}}\mathcal{L}_{\text{FD}} + \lambda_{\text{AE}}\mathcal{L}_{\text{AE}}$$

In practice, we find that applying the flow decoding loss with a non-zero λ_{FD} and backpropagating through the ODE solving steps is critical for successfully training VITA policies. We ablate the effect of λ_{FD} in Figure 5. Furthermore, we observe that using a variational objective for the action autoencoder yields performance comparable to its non-variational counterpart. Since the vision encoder is also not constrained by a variational objective, VITA does not make any specific assumptions about either the source or target distributions.

5 Experiments

We evaluate VITA on the ALOHA bi-manual manipulation benchmark [22, 23], and use simulation environments and datasets provided by AV-ALOHA [22]. Built upon the original ALOHA platform, AV-ALOHA introduces an additional

7-DOF arm equipped with an active vision camera that dynamically adjusts its viewpoint during task execution, which is more challenging due to larger action spaces and non-stationary observation dynamics. The two primary manipulation arms are both 6-DoF plus a gripper, resulting in a total action space of 21 dimensions when accounting for all three arms. We evaluate VITA across 5 simulated tasks (Figure 3) and 2 real-world tasks (Figure 4).

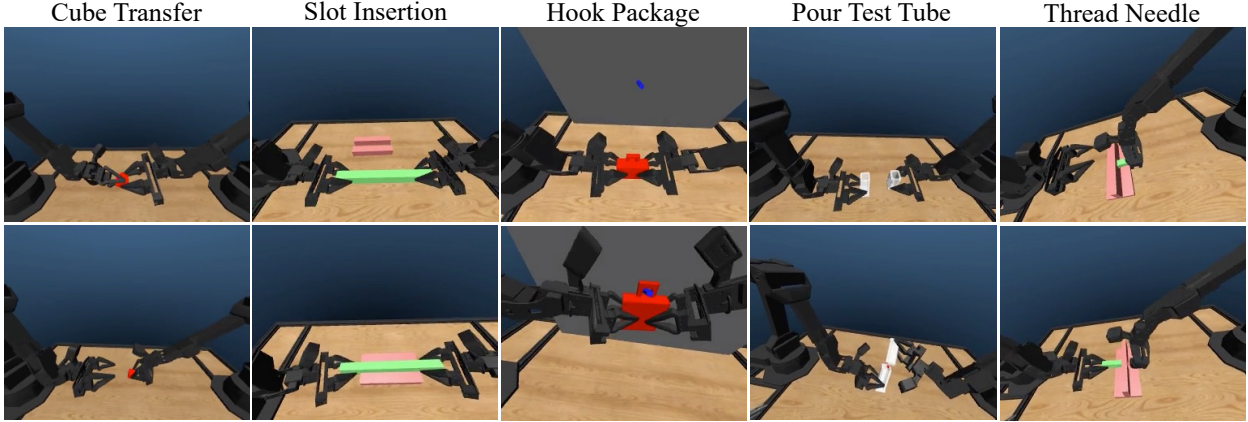


Figure 3: An illustration of five simulation AV-ALOHA tasks, CubeTransfer, SlotInsertion, HookPackage, PourTestTube, and ThreadNeedle.

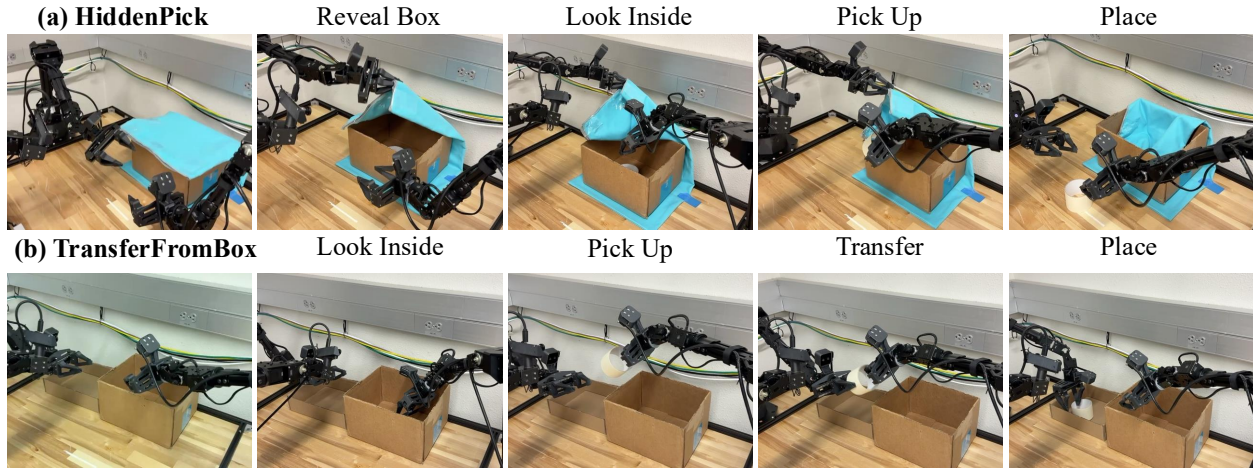


Figure 4: An illustration of two challenging real-world AV-ALOHA tasks, HiddenPick, and TransferFromBox. The pictures are taken from autonomous rollouts by the VITA policy.

Simulated Experiments. We use 5 AV-ALOHA tasks, as depicted in Figure 3, and PushT. Each task has 100-200 demonstrations. AV-ALOHA demonstrations are collected by human experts in simulation using VR headsets; and we use the left eye image as the input. VITA was trained at 25/3 FPS. The action chunk size is 16, and we use the first 8 actions for execution [30].

Real-World Experiments. Two AV-ALOHA real tasks are depicted in Figure 4. We use 50 demonstrations per task for training. For simulated experiments. All the demonstrations are collected by human experts via VR headsets and controllers [22]. In all experiments, we use the left image from the stereo active vision camera as input. VITA was trained at 11 FPS, then linearly interpolated to 33 FPS for deployment on the robot. The action chunk size is also 16, and we use the first 8 actions for execution.

5.1 Implementation

Flow Matcher [18, 45]. To define the probability path and velocity field between the latent distributions, we employ the OT-CFM [46], a conditional flow matching method based on optimal transport (OT). We use six sampling steps to solve numerical ODEs for both flow matching baselines, and VITA.

Vision Encoder. We use a light-weight ResNet-18 [47] as the vision encoder for all the baselines, and VITA. Specifically, we extract the flattened 512-dimensional feature vector after the average pooling layer as the visual representations for VITA. The 1D representation simplifies the flow matching network since the target distribution shares the same shape, and VITA noise-free flow matching can be parameterized with simple MLPs.

VITA Training & Evaluation. For both simulated and real-world experiments, we train the VITA policy on each task for 50,000 gradient steps with a batch size of 128. In simulation, the policy is evaluated every 500 training steps; each evaluation contains 50 episodes. We report the highest success rates for VITA and baselines in Table 1. For real-world tasks, we randomly select 3 checkpoints after convergence, evaluate for 20 episodes per checkpoint, and report the best success rates in Table 2.

Baselines Selection. We compare VITA against several state-of-the-art generative policies, including flow matching (FM) policy [28], diffusion policy (DP)[10], and action chunking transformer (ACT)[26]. We follow the ACT and DP implementation in the LeRobot codebase. In practice, we found DP requires many more training steps than flow matching, and ACT yields sub-optimal performance on most tasks; therefore, we increased training steps to 100,000 for both DP and ACT, and then report the best success rates. For DP, each inference takes 100 DDPM steps [10]. We evaluate both the task performance and inference efficiency of VITA relative to these baselines in Section 5.2.

5.2 Performance & Efficiency

Success Rates. We compare the success rates of VITA against other state-of-the-art conditional generative policies on 6 simulation tasks, including 5 AV-ALOHA tasks (illustrated in Figure 3) with 21D actions for 3 arms, and a PushT task with 2D positional actions. The simulation results are shown in Table 1. We also verify the effectiveness of VITA in real-world settings on two challenging AV-ALOHA [22] tasks (illustrated in Figure 4). The real-world experiment results are shown in Table 2.

VITA consistently outperforms or matches state-of-the-art generative policies across all simulation tasks, as shown in Table 1. ACT exhibits sub-optimal performance even after convergence, while DP requires significantly more training steps than VITA or FM and still remains sub-optimal despite extended training. VITA also demonstrates strong performance on challenging real-world tasks, as shown in Table 2. Examples of autonomous rollouts are illustrated in Figure 4, showcasing the high precision of vision-to-action flow in real-world manipulation tasks involving high-dimensional visual inputs and large action spaces.

Table 1: Task success rates (SR %) across different policies on 5 AV-ALOHA tasks and PushT. Best results are in **bold**.

Task	VITA	FM	DP	ACT
ThreadNeedle	92	88	0	52
SlotInsertion	82	80	20	50
PourTestTube	80	84	6	14
HookPackage	82	72	12	22
CubeTransfer	100	100	76	98
PushT	88	84	80	30

Table 2: Success rates (SR %) of VITA on real-world AV-ALOHA tasks. We report SRs of sequential subtasks for each task.

Task	Subtask	SR (%)
HiddenPick	Reveal	20/20
	Pick	13/20
	Place	13/20
TransferFromBox	Pick	20/20
	Transfer	19/20
	Place	18/20

Efficiency. The VITA policy is highly efficient due to its architectural simplicity. The core components used during inference—the flow matching network and the action decoder—are both lightweight, MLP-only networks. The vision

and action representations are both 1D, further reducing time and space overhead. In total, our model contains only 31M parameters, including the ResNet-18, a vision encoder widely adopted in existing works [13, 10].

We benchmark the inference latency and policy throughput of VITA and compare it against conventional flow matching policy baselines. We implement two different flow matching parameterizations, including diffusion transformer [2], and U-Net [25], and three different conditioning mechanisms, including AdaLN [2], cross-attention [48], and FiLM [31], as the baselines.

FM and DP are typically parameterized using U-Nets [25] or diffusion transformers (DiTs) [2], and are trained to predict velocity fields or noise at each denoising step. While U-Nets and DiTs are highly expressive, they are computationally expensive, posing a significant drawback for real-world robotic deployments that require low-latency inference. In addition, these baselines universally incorporate extra conditioning mechanisms, such as cross-attention [48, 20, 30], AdaLN [20], or FiLM [10], further increasing both inference time and memory footprint.

With a control frequency of 25/3 Hz, our MLP-only VITA policy achieves an inference time of 0.22 ms. In contrast, a comparable flow matching policy built on transformers exhibits a significantly higher latency from 0.33 ms to 0.51 ms and more model parameters. A detailed breakdown of these efficiency metrics is provided in Table 3.

Table 3: Comparison of policy latency and throughput between VITA and conventional flow matching and diffusion policies.

Model	Conditioning	Architecture	Num of Params	Latency (ms/chunk)	Throughput (chunk/s)
VITA	N/A	MLP	31.09M	0.2215	4455.46
FM (S)	AdaLN	DiT	31.16M	0.3307	3027.57
FM (L)	AdaLN	DiT	50.06M	0.4591	2180.38
FM (S)	Cross-Attn	DiT	29.06M	0.5102	1961.66
FM	FiLM	U-Net	84.05M	0.3650	2742.99
Diffusion	FiLM	U-Net	264.66M	368.86	2.71
ACT	Cross-Attn	Transformer	51.59M	3.81	279.58

5.3 Dimensionality Matching for Vision-to-Action Flow

A constraint of flow matching is that the source and target must have identical shapes. In visuomotor contexts, the visual latent representations (z_0) are typically much higher-dimensional than raw action chunks (A). A naive solution would be to down-sample the visual representation to match the action dimensionality, which, nevertheless, leads to significant information loss and poor performance, particularly when the dimensional gap is large.

Table 4: Task SR (%) on ThreadNeedle with different action upsampling strategies.

Up-sampling Strategy	SR (%)
Matrix Transform	0
Action Autoencoder (VITA)	92

Therefore, we adopt the opposite strategy: we map the raw action chunks into a higher-dimensional latent space that matches the dimensionality of the visual latent representations. While a simple linear transformation (e.g., using an invertible matrix) could achieve this up-sampling, our experiments show that action representations produced by such transformations are insufficient for learning reasonable policies. We found that learning well-structured action latent spaces via autoencoders as the target distributions for flow matching can be crucial for the success of vision-to-action flow. We develop an action encoder (\mathcal{E}_a), which does not simply remap dimensions, but also learns structured latent action spaces, making the complex flow from vision to action more tractable.

5.4 Ablation of Flow Latent Decoding

We investigate the importance of the flow latent decoding loss (\mathcal{L}_{FD}) for effectively training VITA policies. Recall that the flow network v_θ learns to transport the visual latent representation $z_0 = \mathcal{E}_v(O)$ to a predicted latent action representation \hat{z}_1 by integrating over the learned velocity field:

$$\hat{z}_1 = z_0 + \int_0^1 v_\theta(z_t, t) dt.$$

During inference, we obtain \hat{z}_1 by numerically solving this ODE using an Euler solver. However, during training, the flow matching loss \mathcal{L}_{FM} supervises velocity predictions only at randomly sampled intermediate time steps, aiming to approximate the ideal transport dynamics between latent representations. This indirect supervision introduces a potential gap: the flow network is trained without direct feedback from the final decoded action quality. As a result, the latent actions generated via ODE integration at inference may not decode into meaningful actions. To bridge this gap, we propose two direct supervision strategies for \hat{z}_1 : 1) the **Reconstruction Loss**, which decodes \hat{z}_1 into the original action space and computes the reconstruction error against the ground-truth action A , i.e., $\mathcal{L}_{FD} = \|\mathcal{D}_a(\hat{z}_1) - A\|$; and 2) the **Consistency Loss**, which directly aligns the predicted latent action with the encoded latent target $z_1 = \mathcal{E}_a(A)$, using $\|\hat{z}_1 - z_1\|$.

As shown in Figure 5, without any flow decoding supervision (i.e., $\lambda_{FD} = 0$) and gradients through ODE steps, the model fails entirely to learn a meaningful policy. In contrast, applying flow latent decoding, especially via reconstruction, is critical for effective learning and achieving high performance. The consistency loss provides a weaker signal, resulting in slower convergence and slightly lower success rates. These results highlight the necessity of propagating gradients from the action latent space through the ODE solving steps of flow matching.

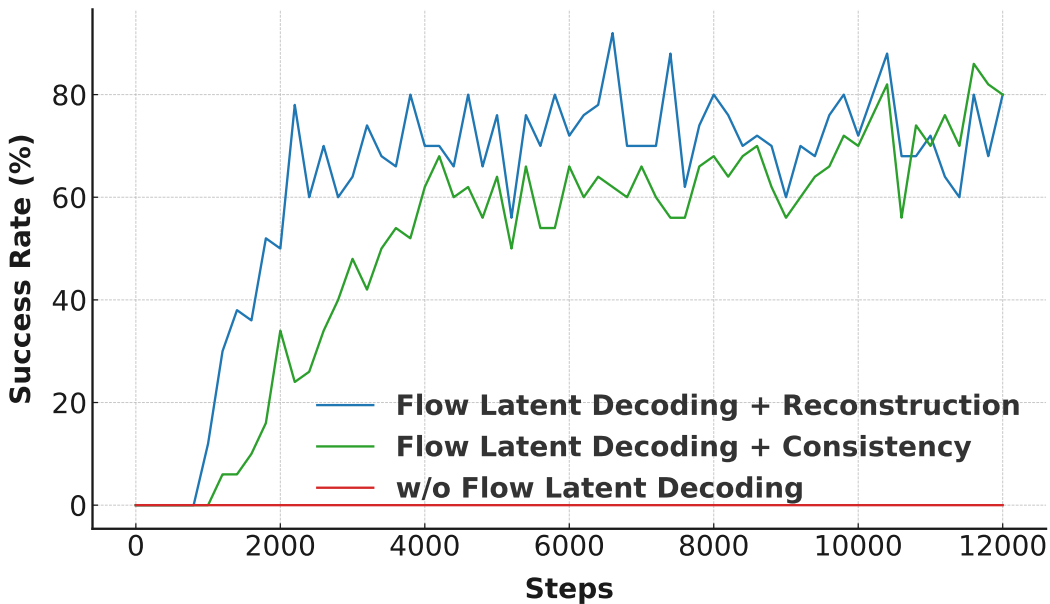


Figure 5: Ablation study on flow latent decoding. We compare different objective functions for supervising the predicted action latent \hat{z}_1 obtained by solving the flow ODE. The reconstruction loss decodes \hat{z}_1 and compares it to the ground-truth action A , while the consistency loss directly aligns \hat{z}_1 with the encoded action latent $z_1 = \mathcal{E}_a(A)$. Without any flow decoding loss, the model fails to learn.

6 Conclusion

In this work, we introduced VITA, a simple, efficient, and high-performing visuomotor policy. VITA generates actions in a noise-free manner and directly evolves latent visual representations into latent actions. By leveraging latent image representations as the flow’s source distribution, VITA eliminates the need for complex conditioning mechanisms such as cross-attention, significantly simplifying model architecture and enhancing efficiency. Furthermore, VITA employs 1D representations for both latent images and actions, and therefore, enables an MLP-only architecture for the flow matching network and action decoder. Two key designs are critical to VITA’s success —structuring the latent action space using an action autoencoder and enabling gradient propagation of flow latent decoding losses across ODE solving steps —allowing VITA to effectively bridge latent images and latent actions in a fully end-to-end manner from scratch. Extensive experiments demonstrate that VITA achieves state-of-the-art performance on challenging ALOHA bi-manual manipulation tasks in both simulated and real-world environments. VITA can generate around 4,500 action chunks (with a chunk size of 16) per second, reducing inference latency by approximately 50% compared to flow matching using adaptive layer normalization for conditioning, and by 130% compared to flow matching using cross-attention.

References

- [1] Robin Rombach, Andreas Blattmann, Dominik Lorenz, Patrick Esser, and Björn Ommer. High-resolution image synthesis with latent diffusion models. In Proceedings of the IEEE/CVF conference on computer vision and pattern recognition, pages 10684–10695, 2022.
- [2] William Peebles and Saining Xie. Scalable diffusion models with transformers. In Proceedings of the IEEE/CVF international conference on computer vision, pages 4195–4205, 2023.
- [3] Nanye Ma, Mark Goldstein, Michael S Albergo, Nicholas M Boffi, Eric Vanden-Eijnden, and Saining Xie. Sit: Exploring flow and diffusion-based generative models with scalable interpolant transformers. In European Conference on Computer Vision, pages 23–40. Springer, 2024.
- [4] Qihao Liu, Xi Yin, Alan Yuille, Andrew Brown, and Mannat Singh. Flowing from words to pixels: A framework for cross-modality evolution. arXiv preprint arXiv:2412.15213, 2024.
- [5] Ju He, Qihang Yu, Qihao Liu, and Liang-Chieh Chen. Flowtok: Flowing seamlessly across text and image tokens. arXiv preprint arXiv:2503.10772, 2025.
- [6] Lvmin Zhang, Anyi Rao, and Maneesh Agrawala. Adding conditional control to text-to-image diffusion models. In Proceedings of the IEEE/CVF international conference on computer vision, pages 3836–3847, 2023.
- [7] Jonathan Ho, Tim Salimans, Alexey Gritsenko, William Chan, Mohammad Norouzi, and David J Fleet. Video diffusion models. Advances in Neural Information Processing Systems, 35:8633–8646, 2022.
- [8] Xin Li, Wenqing Chu, Ye Wu, Weihang Yuan, Fanglong Liu, Qi Zhang, Fu Li, Haocheng Feng, Errui Ding, and Jingdong Wang. Videogen: A reference-guided latent diffusion approach for high definition text-to-video generation. arXiv preprint arXiv:2309.00398, 2023.
- [9] Yang Jin, Zhicheng Sun, Ningyuan Li, Kun Xu, Hao Jiang, Nan Zhuang, Quzhe Huang, Yang Song, Yadong Mu, and Zhouchen Lin. Pyramidal flow matching for efficient video generative modeling. arXiv preprint arXiv:2410.05954, 2024.
- [10] Cheng Chi, Zhenjia Xu, Siyuan Feng, Eric Cousineau, Yilun Du, Benjamin Burchfiel, Russ Tedrake, and Shuran Song. Diffusion policy: Visuomotor policy learning via action diffusion. The International Journal of Robotics Research, page 02783649241273668, 2023.
- [11] Allen Z Ren, Justin Lidard, Lars L Ankile, Anthony Simeonov, Pulkit Agrawal, Anirudha Majumdar, Benjamin Burchfiel, Hongkai Dai, and Max Simchowitz. Diffusion policy policy optimization. arXiv preprint arXiv:2409.00588, 2024.
- [12] Dechen Gao, Hang Wang, Hanchu Zhou, Nejb Ammar, Shatadal Mishra, Ahmadreza Moradipari, Iman Soltani, and Junshan Zhang. In-ril: Interleaved reinforcement and imitation learning for policy fine-tuning. arXiv preprint arXiv:2505.10442, 2025.
- [13] Yue Su, Xinyu Zhan, Hongjie Fang, Han Xue, Hao-Shu Fang, Yong-Lu Li, Cewu Lu, and Lixin Yang. Dense policy: Bidirectional autoregressive learning of actions. arXiv preprint arXiv:2503.13217, 2025.
- [14] Qinglun Zhang, Zhen Liu, Haoqiang Fan, Guanghui Liu, Bing Zeng, and Shuaicheng Liu. Flowpolicy: Enabling fast and robust 3d flow-based policy via consistency flow matching for robot manipulation. In Proceedings of the AAAI Conference on Artificial Intelligence, volume 39, pages 14754–14762, 2025.
- [15] Quentin Rouxel, Andrea Ferrari, Serena Ivaldi, and Jean-Baptiste Mouret. Flow matching imitation learning for multi-support manipulation. In 2024 IEEE-RAS 23rd International Conference on Humanoid Robots (Humanoids), pages 528–535. IEEE, 2024.
- [16] Max Braun, Noémie Jaquier, Leonel Rozo, and Tamim Asfour. Riemannian flow matching policy for robot motion learning. In 2024 IEEE/RSJ International Conference on Intelligent Robots and Systems (IROS), pages 5144–5151. IEEE, 2024.
- [17] Kevin Black, Noah Brown, Danny Driess, Adnan Esmail, Michael Equi, Chelsea Finn, Niccolo Fusai, Lachy Groom, Karol Hausman, Brian Ichter, et al. $\pi 0$: A vision-language-action flow model for general robot control, 2024. URL <https://arxiv.org/abs/2410.24164>.
- [18] Yaron Lipman, Ricky T. Q. Chen, Heli Ben-Hamu, Maximilian Nickel, and Matt Le. Flow matching for generative modeling, 2023.
- [19] Jascha Sohl-Dickstein, Eric Weiss, Niru Maheswaranathan, and Surya Ganguli. Deep unsupervised learning using nonequilibrium thermodynamics. In International conference on machine learning, pages 2256–2265. pmlr, 2015.
- [20] Sudeep Dasari, Oier Mees, Sebastian Zhao, Mohan Kumar Srirama, and Sergey Levine. The ingredients for robotic diffusion transformers. arXiv preprint arXiv:2410.10088, 2024.

- [21] Qihao Liu, Adam Kortylewski, Yutong Bai, Song Bai, and Alan Yuille. Discovering failure modes of text-guided diffusion models via adversarial search. [arXiv preprint arXiv:2306.00974](#), 2023.
- [22] Ian Chuang, Andrew Lee, Dechen Gao, M Naddaf-Sh, Iman Soltani, et al. Active vision might be all you need: Exploring active vision in bimanual robotic manipulation. [arXiv preprint arXiv:2409.17435](#), 2024.
- [23] Zipeng Fu, Tony Z Zhao, and Chelsea Finn. Mobile aloha: Learning bimanual mobile manipulation using low-cost whole-body teleoperation. In [8th Annual Conference on Robot Learning](#), 2024.
- [24] Tony Z Zhao, Jonathan Tompson, Danny Driess, Pete Florence, Kamyar Ghasemipour, Chelsea Finn, and Ayzaan Wahid. Aloha unleashed: A simple recipe for robot dexterity. [arXiv preprint arXiv:2410.13126](#), 2024.
- [25] Olaf Ronneberger, Philipp Fischer, and Thomas Brox. U-net: Convolutional networks for biomedical image segmentation. In [International Conference on Medical image computing and computer-assisted intervention](#), pages 234–241. Springer, 2015.
- [26] Tony Z Zhao, Vikash Kumar, Sergey Levine, and Chelsea Finn. Learning fine-grained bimanual manipulation with low-cost hardware. [arXiv preprint arXiv:2304.13705](#), 2023.
- [27] Andrew Lee, Ian Chuang, Ling-Yuan Chen, and Iman Soltani. Interact: Inter-dependency aware action chunking with hierarchical attention transformers for bimanual manipulation. [arXiv preprint arXiv:2409.07914](#), 2024.
- [28] Fan Zhang and Michael Gienger. Affordance-based robot manipulation with flow matching. [arXiv preprint arXiv:2409.01083](#), 2024.
- [29] Letian Fu, Huang Huang, Gaurav Datta, Lawrence Yunliang Chen, William Chung-Ho Panitch, Fangchen Liu, Hui Li, and Ken Goldberg. In-context imitation learning via next-token prediction. [arXiv preprint arXiv:2408.15980](#), 2024.
- [30] Zhefei Gong, Pengxiang Ding, Shangke Lyu, Siteng Huang, Mingyang Sun, Wei Zhao, Zhaoxin Fan, and Donglin Wang. Carp: Visuomotor policy learning via coarse-to-fine autoregressive prediction. [arXiv preprint arXiv:2412.06782](#), 2024.
- [31] Ethan Perez, Florian Strub, Harm De Vries, Vincent Dumoulin, and Aaron Courville. Film: Visual reasoning with a general conditioning layer. In [Proceedings of the AAAI conference on artificial intelligence](#), volume 32, 2018.
- [32] Jonathan Ho, Ajay Jain, and Pieter Abbeel. Denoising diffusion probabilistic models. [Advances in neural information processing systems](#), 33:6840–6851, 2020.
- [33] Xingchao Liu, Chengyue Gong, and Qiang Liu. Flow straight and fast: Learning to generate and transfer data with rectified flow, 2022.
- [34] Alexander Tong, Nikolay Malkin, Kilian Fatras, Lazar Atanackovic, Yanlei Zhang, Guillaume Huguët, Guy Wolf, and Yoshua Bengio. Simulation-free schrödinger bridges via score and flow matching, 2024.
- [35] Patrick Esser, Sumith Kulal, Andreas Blattmann, Rahim Entezari, Jonas Müller, Harry Saini, Yam Levi, Dominik Lorenz, Axel Sauer, Frederic Boesel, et al. Scaling rectified flow transformers for high-resolution image synthesis, 2024. [URL https://arxiv.org/abs/2403.03206](https://arxiv.org/abs/2403.03206), 2.
- [36] Qihao Liu, Zhanpeng Zeng, Ju He, Qihang Yu, Xiaohui Shen, and Liang-Chieh Chen. Alleviating distortion in image generation via multi-resolution diffusion models and time-dependent layer normalization. [Advances in Neural Information Processing Systems](#), 37:133879–133907, 2024.
- [37] Sucheng Ren, Qihang Yu, Ju He, Xiaohui Shen, Alan Yuille, and Liang-Chieh Chen. Flowar: Scale-wise autoregressive image generation meets flow matching. [arXiv preprint arXiv:2412.15205](#), 2024.
- [38] Songming Liu, Lingxuan Wu, Bangguo Li, Hengkai Tan, Huayu Chen, Zhengyi Wang, Ke Xu, Hang Su, and Jun Zhu. Rdt-1b: a diffusion foundation model for bimanual manipulation. [arXiv preprint arXiv:2410.07864](#), 2024.
- [39] Michael S Albergo and Eric Vanden-Eijnden. Building normalizing flows with stochastic interpolants. [arXiv preprint arXiv:2209.15571](#), 2022.
- [40] Alexander Tong, Nikolay Malkin, Kilian Fatras, Lazar Atanackovic, Yanlei Zhang, Guillaume Huguët, Guy Wolf, and Yoshua Bengio. Simulation-free schrödinger bridges via score and flow matching. [arXiv preprint arXiv:2307.03672](#), 2023.
- [41] Johannes S Fischer, Ming Gui, Pingchuan Ma, Nick Stracke, Stefan A Baumann, and Björn Ommer. Boosting latent diffusion with flow matching. [arXiv preprint arXiv:2312.07360](#), 2023.
- [42] Xingchao Liu, Chengyue Gong, and Qiang Liu. Flow straight and fast: Learning to generate and transfer data with rectified flow. [arXiv preprint arXiv:2209.03003](#), 2022.
- [43] Xingchao Liu, Chengyue Gong, and Qiang Liu. Flow straight and fast: Learning to generate and transfer data with rectified flow. [arXiv preprint arXiv:2209.03003](#), 2022.

- [44] Diederik P Kingma, Max Welling, et al. Auto-encoding variational bayes, 2013.
- [45] Alexander Tong, Nikolay Malkin, Kilian Fatras, Lazar Atanackovic, Yanlei Zhang, Guillaume Huguet, Guy Wolf, and Yoshua Bengio. Simulation-free schrödinger bridges via score and flow matching. [arXiv preprint arXiv:2307.03672](#), 2023.
- [46] Alexander Tong, Kilian Fatras, Nikolay Malkin, Guillaume Huguet, Yanlei Zhang, Jarrid Rector-Brooks, Guy Wolf, and Yoshua Bengio. Improving and generalizing flow-based generative models with minibatch optimal transport. [arXiv preprint arXiv:2302.00482](#), 2023.
- [47] Kaiming He, Xiangyu Zhang, Shaoqing Ren, and Jian Sun. Deep residual learning for image recognition. In [Proceedings of the IEEE conference on computer vision and pattern recognition](#), pages 770–778, 2016.
- [48] Ashish Vaswani, Noam Shazeer, Niki Parmar, Jakob Uszkoreit, Llion Jones, Aidan N Gomez, Łukasz Kaiser, and Illia Polosukhin. Attention is all you need. [Advances in neural information processing systems](#), 30, 2017.